Streamer and Surface Charge Dynamics in Non-Uniform Air Gaps with a Dielectric Barrier

Hans Kristian Meyer and **Frank Mauseth**
NTNU – Norwegian University of Science and Technology
Department of Electric Power Engineering
Trondheim, Norway

Robert Marskar and **Atle Pedersen**
SINTEF Energy Research
Trondheim, Norway

Andreas Blaszczyk
ABB Ltd.
Baden-Dättwil, Switzerland

ABSTRACT

Streamer behaviour near dielectric surfaces is an important characteristic of air-solid electrical insulation systems. Accurate predictions are important for dielectric design, but dynamic aspects such as surface charging during streamer propagation are not well understood. A drift-diffusion model is used here to simulate positive streamer behaviour in non-uniform fields. The 2D-planar simulation domain includes air gaps between a tip of a HV electrode and a dielectric barrier laying on a grounded plane. The resulting surface charge distributions approach saturation charge conditions, i.e. zero normal electric field on the air side of the boundary. Such charging behaviour was also reported in lightning impulse (LI) experiments. The simulations are also aligned with empirical streamer propagation range estimates. It is demonstrated that saturation charge levels are reachable within a few tens of nanoseconds of exposure to positive streamer channels. Ion drift is shown to be the dominating mechanism of surface charging during positive streamer propagation, although photoemission also plays an important role. Discharge suppression by streamer-deposited surface charge is also demonstrated. Furthermore, the influence of back discharges at the LI tail on the surface charge distribution is shown. Simulating realistic streamer surface charging behaviour with arbitrary electrode and dielectric shapes is an important step toward first principles discharge prediction models.

Index Terms — **gas discharges, gas insulation, dielectrics, surface charging, air gaps, surface discharges, electron emission, plasma simulation**

1 INTRODUCTION

PREDICTING discharge behaviour is important in many high voltage applications. Charging of dielectric surfaces may affect the insulation properties of a high voltage device significantly. Recent experiments on rod-barrier-plane air gaps under lightning impulse voltage (LI) have shown that charging by streamers can be estimated with a zero (saturation) or equalized normal electric field at the charged surface [1]. Such conditions can be computed with electrostatic simulations. They can therefore be used to evaluate surface charging during voltage tests in complex geometries [2]. If surface charge effects are predictable, they can be used to the benefit of the insulation system. It is, for example, conceivable that surface charging by streamers may inhibit the secondary discharge phenomena necessary for LI breakdown [3-5]. Such aspects can only be explored in detail with dynamic simulation models and experiments.

The dynamics of surface charging by streamers are in general not well known. The streamer-exposed surface is charged by drifting ions or electrons from the streamer channel and by electron emission processes from the dielectric surface [5]. These mechanisms occur in different regions of the streamer and on different time scales, and their relative importance is not clear. The aim of this work is therefore to investigate, using drift-diffusion simulations, the dynamics of

Manuscript received on 12 November 2018, in final form 12 February 2019, accepted 14 February 2019. Corresponding author: H.K. Meyer.

streamer-dielectric interaction in short non-uniform air gaps. Specifically, to clarify the time scale, range and mechanisms of surface charging during positive surface streamer propagation. Also, to understand how saturation charge levels can be reached during a LI. Another aim is to demonstrate discharge suppression by streamer-deposited surface charge, as this is an important insulation system feature. Furthermore, it is an aim to reproduce the influence of back discharges at the LI tail on surface charge distributions [1,6].

Comparisons of drift-diffusion models with experiments are few when it comes to streamer-dielectric interaction and surface charge accumulation [7,8]. An overarching goal of this work is therefore to demonstrate that drift-diffusion models can reproduce experimentally observed characteristics of streamer discharges near dielectrics.

2 SIMULATIONS OF STREAMERS NEAR DIELECTRIC SURFACES IN AIR

2.1 STREAMER DISCHARGES

If an electron avalanche grows to a critical size (10^6-10^8 electrons), its internal field can sustain discharge processes in relatively low background fields. The field strength around the space charge head is then high enough ($E_{cr} \approx 2.6$ kV/mm for 1 bar air) to support further electron avalanche processes in the vicinity [9]. These so-called streamer discharges can be either cathode-directed (positive) or anode-directed (negative). For positive streamers, the electrons from the secondary avalanches are neutralized by positive charges in the streamer head, leaving behind new positive charge a little closer to the cathode. The secondary electrons are generated by impact ionization and photo-ionization. As the process continues, the space charge wave propagates until it meets the cathode or until the electric field is not able to sustain the ionization processes.

Electron avalanches from negative streamers start from the negative space charge head and propagate toward the anode, into a lower field region. Negative streamers therefore require higher background fields in air than positive ones to propagate. Detailed information on characteristics of negative streamers, which are not the focus of this paper except of back discharges discussed in Section 5.6, can be found in [10].

2.2 DRIFT-DIFFUSION MODELING OF STREAMERS

Drift-diffusion models are widely used to simulate streamers in air [4, 7, 8, 11-19]. They are based on a set of drift-diffusion-reaction continuity equations describing the evolution of each type of charged species i:

$$\frac{\partial n_i}{\partial t} + \nabla \cdot (\mathbf{v}_i n_i - D_i \nabla n_i) = S_i, \tag{1}$$

where n_i is the density of the charged species i. Three species are used in this work: electrons (i=e), positive and negative ions $i = \pm$. $\mathbf{v}_i$ is the drift velocity and D_i the diffusion coefficient. Ion diffusion is usually neglected as it is slow on streamer propagation time scales. The expressions for source terms S_i are given below. If it is assumed that streamer channel currents are low, magnetic fields can be disregarded, and the remaining Maxwell equation for the evolution of the electromagnetic field is Poisson's equation

$$\nabla \cdot (-\epsilon \nabla \Phi) = \rho_f, \tag{2}$$

where Φ is electric potential, ε is permittivity, and ρ_f is the free charge density. The way used to incorporate surface charges in Equation (2) is explained in [16].

Additionally, solutions to a set of radiative transfer equations (RTE) are approximated with the Eddington and three-group approximation [20] to model photo-ionization.

Equations (1) and (2) and the RTEs are coupled through S_i, D_i, and $\mathbf{v}_i$ with the streamer plasma kinetics model described in [11], which has been widely used (e.g. in [15,19]). The source terms S_i are given by:

$$\begin{aligned} S_e &= S_{ph.} + n_e \alpha \,|\, \mathbf{v}_e \,|\, - n_e \eta \,|\, \mathbf{v}_e \,|\, - n_e n_+ \beta \\ S_+ &= S_{ph.} + n_e \alpha \,|\, \mathbf{v}_e \,|\, - n_e n_+ \beta - n_- n_+ \beta \\ S_- &= n_e \eta \,|\, \mathbf{v}_e \,|\, - n_- n_+ \beta \end{aligned} \tag{3}$$

where α, β, and η are ionization, attachment, and recombination coefficients respectively, for which simplified empirical expressions are given in [11]. Note for example that the same β is used for ion-ion and electron-ion recombination. More accurate reaction rates relevant to streamers in air can be found in e.g. [21] and references therein. $S_{ph.}$ is the photo-ionization source term, see [20] for details.

A charge-neutral uniform density of positive ions and electrons, 10^{10} m^{-3}, which is a typical level inside buildings [21], is applied as a simplified initial condition (same approach as in [7, 12, 18]). Other typical initial conditions in such simulations are constant background ionization rates [15], stochastic charge carrier densities [17] or initial plasma clouds [20–22]. Either way, the initial conditions used here are justified since the goal of computation is the surface charging and not the initial stage of the discharge. One should nevertheless keep in mind that the measured surface charge shows statistical deviations when repeating the same experiment (see measured surface charge in Figure 1). One of the reasons explaining such a behavior may be initial conditions. At the electrodes, there is a free outflow of charged species.

2.3 DIELECTRIC SURFACES IN DRIFT-DIFFUSION MODELS

As the streamer propagates near a dielectric surface, there is a net charge flux (current density)

$$J_\sigma = d\sigma / dt = q_e (F_e - F_+ + F_-) \tag{4}$$

into the surface. J_σ is integrated over time and becomes surface charge σ. q_e is the electron charge, F_e, F_+, and F_- are fluxes of charged species onto the surface. The software (see section 2.4) uses embedded boundaries, so the fluxes are extrapolated from the air to the surface (see [16] for details). Charged species are not emitted from the surface if the extrapolated flux points out of the dielectric:

$$\begin{aligned} F_+ &= \max(0, \tilde{F}_+) \\ F_- &= \max(0, \tilde{F}_-) \\ F_e &= \max(0, \tilde{F}_e) - A(\gamma F_{ph} + \kappa F_+) \\ A &= \begin{cases} 1, & \text{if } \mathbf{E} \cdot \mathbf{n} \le 0 \\ 0, & \text{otherwise} \end{cases} \end{aligned} \tag{5}$$

Here $\tilde{F}_+$, $\tilde{F}_-$, and $\tilde{F}_e$ are linearly extrapolated fluxes from the air to the surface, $\mathbf{E} = -\nabla\Phi$ is the electric field and $\mathbf{n}$ is the surface normal pointing into the air. F_{ph} is the photon flux into the surface (the method of calculating photon fluxes is based on the gradient of the radiative density [16]). Two electron emission mechanisms are implemented in the electron flux F_e: photoemission (γ electrons released per incident photon) and positive ion bombardment (κ electrons released per incident positive ion). These only contribute when the electric field points into the dielectric, hence the conditional A. Emission mechanisms contribute to surface charging, as every emitted electron leaves behind an electron hole, which is equivalent to an immobile, positive surface charge in the model.

Positive and negative ions are not emitted from the surface in the model. If the extrapolated flux is positive, the respective charge carriers are flowing onto the dielectric (becoming surface charge according to Equation (4)). If, on the other hand, the extrapolated flux is negative, the respective charge carriers would normally flow out of surface. To avoid such emission, max() functions are used in Equation (5). The charge exchange at the dielectric surface in the model is limited to charged species drifting onto the dielectric, and emission of electrons due to photon and positive ion bombardment. For ion bombardment, a high value of $\kappa = 0.1$ is used here as in [7, 18]. A low value of $\kappa = 10^{-4}$ was also briefly tried. This parameter does not alter the streamer characteristics in the model, but it accelerates the surface charging rate (the surface charging rate is ca. 10 % higher with $\kappa = 0.1$). γ (photoemission efficiency), depends on both the material and gas properties. Experimental data on photoemission from dielectrics is limited, especially in the presence of a discharge. Estimates for γ fall in the large range from 10^{-7} to 1 for polymers (references can be found in [22]). The photoionization model in this work models only UV-photons around 100 nm, as those are considered to be responsible for photoionization in air. Longer wavelength photons may contribute to photoemission from dielectric surfaces in air, but the effect is small as γ decreases with decreasing photon energy. In this study, γ was set to 10^{-6} and 10^{-1} to study its influence on the surface charge accumulation and positive streamer dynamics.

2.4 IMPLEMENTATION AND COMPUTATIONAL RESOURCES

A finite volume code [16] was used for the dynamic simulations. The implementation uses Cartesian cut cell grids to handle material boundaries and adaptive mesh refinement to limit the grid size. The local mesh size is mainly controlled by the relative electric field strength and its gradient in this work. The same refinement criteria as in [16] are used.

Drift-diffusion simulations of streamers in atmospheric air in realistic geometries are computationally demanding. Streamers span several spatial and temporal scales, with typical minimum resolutions in the low or sub µm and ps range when streamers propagate on dielectric surfaces [22]. The main computational bottleneck is the Poisson's equation [17]. 3D simulations with branching (see e.g. [17]) are required to realistically model streamers, but they are currently too computationally expensive for larger domains with sub µm grids and complex geometries. The simulations here were therefore in 2D, and used up to 512 computer cores when the mesh size was 0.61 µm at the finest level and 312.5 µm at the coarsest. The number of cells varied from a few million to 14 million. The minimum time steps were around 0.3-0.6 ps, mainly controlled with the Courant-Friedrichs-Lewy condition (see [16] for details).

3 ENGINEERING SIMULATIONS BASED ON SATURATION CHARGE

Predicting the influence of surface charge on the dielectric strength of gas-insulated high-voltage devices is still outside of the capabilities of drift-diffusion models. Therefore, a simplified approach based on a saturation boundary condition has been suggested as an engineering approach for complex geometries [1, 2]. The saturation is defined by zero normal field on the air side of a dielectric interface:

$$E_{n,air} = 0, \tag{6}$$

whereas the unknown saturation charge σ_{sat} is balanced by the electric flux density on the solid dielectric side

$$\epsilon_{ins} E_{n,ins} - \sigma_{sat} = 0 \tag{7}$$

Here ε_{ins} is the permittivity of the dielectric and $E_{n,ins}$ the normal field inside the dielectric at the gas-dielectric interface.

The region of the surface where this condition is applied is estimated by assuming that the propagation is limited by the maximum streamer range

$$s_r = U / E_{st}, \tag{8}$$

where E_{st} is the background field required for streamer propagation along insulating surfaces in atmospheric air and U is the applied voltage. For positive streamers along insulating surfaces, $E_{st} \approx$ 0.4-0.6 kV/mm [23]. E_{st} = 0.5 kV/mm is used here.

Commercial finite element method (FEM) software

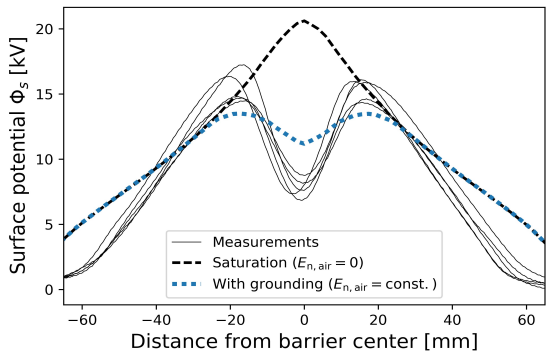

Figure 1 Surface potential measurements on rod-barrier-plane gaps stressed with 35 kV 1.2/50 µs LI [1]. The measured potentials (grey solid lines) are partly close to the predicted saturation (black dashed line based on equations (6)-(8)). The characteristic volcano shape can be explained by back discharges at the LI tail. They can be computed according to [1] by removing a part of the accumulated charge and equalizing the normal electric field (blue dotted line). 2 mm rod radius, tip 10 mm above ground. 5 mm thick polycarbonate barrier resting on the ground plane. 5 independent measurements, surface cleaned and discharged between experiments.

(COMSOL Multiphysics) and an in-house ABB engineering tool called VHVlab based on the boundary element method (BEM) [2] were used to compute saturation charge conditions in this work and in [1]. In [1], the procedure described above (Equations (6)-(8)) was tested with experimental results on rod-barrier-plane gaps under LI (see Figure 1).

4 SIMULATION CASES

Blade-barrier-plane gaps were used for the dynamic and engineering simulations. Since the dynamic code does not support cylindrical coordinates and the 3D code is computationally too heavy, we cannot obtain dynamic results that can be directly compared with the experiments in [1]. Instead, an indirect approach has been applied: for an equivalent 2D-planar arrangement the results of the dynamic code are compared with the results of the experimentally validated engineering codes.

Two simulation geometries were used, see Table 1 and Figure 2. Throughout, the dielectric was 5 mm thick with $\varepsilon_r = 3$, resting on the ground plane and centered. The barrier is assumed to be ideally insulating. The assumption is that on the time scale of the streamer, conduction through the dielectric slab is negligibly slow compared to the conduction in the streamer-ionized air. The barrier edges were rounded with 0.2 mm radius.

A constant potential U was applied in the simulations instead of a 1.2/50 µs LI pulse. The total duration of the simulations was only between 15 and 115 ns. If it is assumed that the first electron avalanche will appear close to the LI peak, the voltage level variation during 115 ns is only a few percent, so a constant potential is a reasonable approximation.

Table 1. Simulation parameters. See also Figure 2.

Parameter	Geometry	
	G1	G2
Domain [mm^2]	40x40	80x20
Blade tip radius [mm]	2	0.5
Blade potential U [kV]	35	14/35
Barrier width [mm]	22	72
Photoemission efficiency γ	10^{-6}/10^{-1}	10^{-6}

5 RESULTS AND DISCUSSION

5.1 COMPARISON WITH SATURATION CHARGE

The drift-diffusion simulations typically show a streamer initiated from the blade tip, propagating vertically, and then hitting the dielectric. It then continues horizontally along the dielectric surface (see illustration in section 5.4, Fig 7). Finally, the streamer propagates around the barrier edge, detaches partly from the surface, and then propagates toward the ground plane. Meanwhile, the surface charge density distribution on the dielectric surface evolves toward saturation levels, see Figure 3.

The streamers in geometry G1 reached the ground plane after around 15.5 ns, whereas the simulations in G2 were stopped before the streamers reached ground. The position of the optical streamer head at the simulation end is indicated in

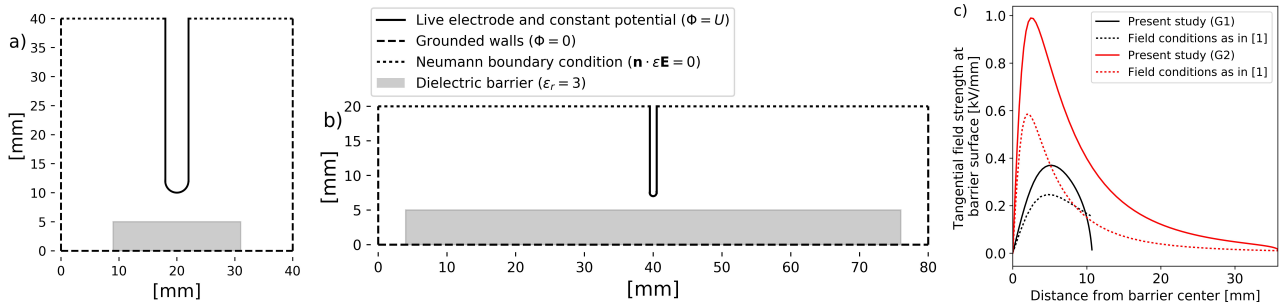

Figure 2 Simulation domains with boundary conditions for the electric field. The simulations are 2D planar, meaning that the dimensions are infinite into and out of the paper. So the geometries are blade-barrier-plane gaps. a) Geometry G1 b) Geometry G2 (See also Table 1). c) distribution of the tangential background field strength E_t along the barrier surface with 35 kV applied to the live electrode. Note: The grounded vertical wall reflects the experimental condition in HV labs. Therefore, we keep the same conditions for both cases in spite of the fact that the computational domain is limited to a rather small area. E_t is higher in the blade-barrier-plane simulations here than in the corresponding rod-barrier-plane gaps in [1]: not due to the reduced distance to vertical grounded walls but because of differences between background field surrounding live electrodes (blade versus rod).

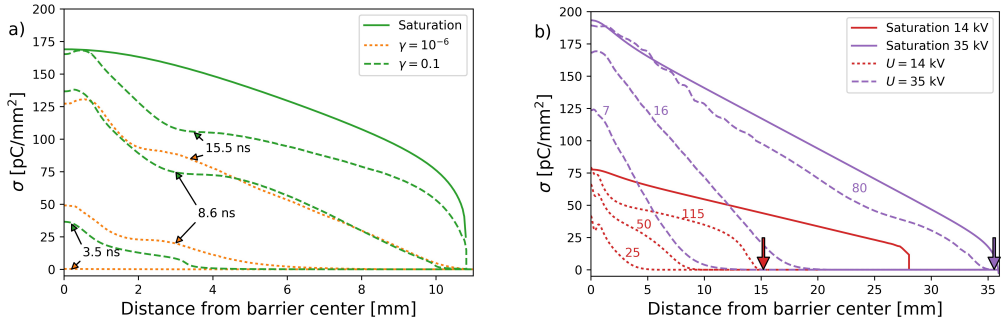

Figure 3 Surface charge density distribution σ (dotted and dashed lines) evolves toward saturation charge σ_{sat} (solid lines) on the dielectric surface. Numerals indicate elapsed simulation time in ns. a) Geometry G1, photoemission increases surface charging rate b) Geometry G2, effect of applied voltage level. Small vertical arrows indicate the optical streamer head position in G2. The simulations in G2 were stopped due to excessive computation time before the streamer reached the edge of the dielectric barrier. The reason is that the streamer slows down in the low-field regions (especially for the 14 kV case). This requires much more time steps that remain small (below 1 ps) and consequently the simulation needs up to a few days on a computer cluster.

Figure 3b. It is the point of the most intense photon production and is obtained from the photon source term.

For the positive ions in the streamer channel to charge the surface up to saturation, the number of positive charge carriers in the streamer channel must exceed the total saturation charge Q_{sat} (negative charge carriers drift away from the dielectric surface and do not contribute to surface charge). The value of Q_{sat} in geometry G1 (Figure 3a) is 2.8 µC/m. so $n_{+,sat} = 1.75 \times 10^{13}$/m positive charge carriers are needed (the values of surface charge and carriers are given here per m due to the 2D planar approximation). Integrating the positive species density in the streamer channel at the time instant in Figure 4a, it contains 4 x 10^{14}/m > $n_{+,sat}$, so there are sufficient charge carriers to reach saturation (ca. 20 times more than needed). Similarly, it was found that there are sufficient charge carriers to reach saturation in the streamer channels in geometry G2.

Charge levels above saturation are also possible, if the electric field distortion from the streamer space charge density (Figure 4b) is substantially higher than the field distortion from the saturation charge density. Most of the streamer channel is a quasi-neutral, i.e. apparently charge neutral, plasma. There are high densities of charge carriers of both polarities in the channel, but they cancel out. However, there is a ca. 20 µm thick layer of space charge partly surrounding the quasi-neutral streamer channel (Figure 4b). All in all, the electric field contribution from the streamer space charge is not high enough to achieve significant super-saturation in the simulations here.

5.1 CHARGING DYNAMICS

The charge carriers must reach and cover the surface within the relevant time scale to charge it. Firstly, the streamer must cross the air gap. The time of crossing depends on the applied field strength (see section 4.4).

As the streamer propagates along the dielectric surface, the comparatively slow positive ions need time to drift onto it. The surface charge decay mechanisms are slow on streamer propagation time scales, so the charge accumulation rate depends mainly on ionization rates, surface emission rates and

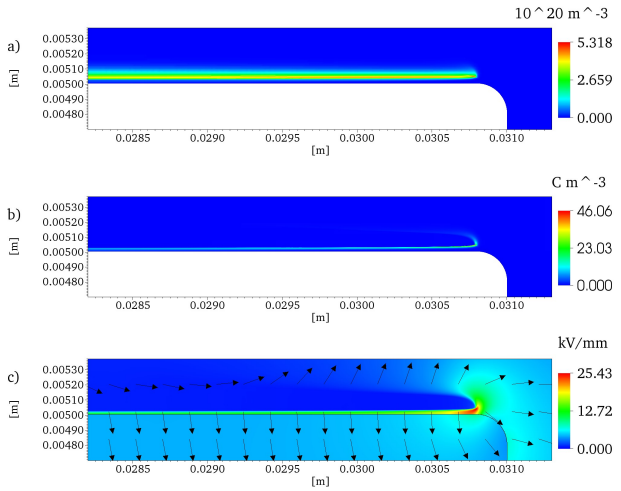

Figure 4 Streamer at the barrier edge in geometry G1 at $t = 11.56$ ns, with $\gamma = 10^{-6}$. a) Density of positive ions in 10^{20} m^{-3} b) Space charge density in Cm^{-3} c) Electric field strength in kV/mm with a few field vectors.

positive ion drift velocities

$$\mathbf{v}_+ = \mu_+ \mathbf{E} = 2.34 \cdot 10^{-4}\ [\mathrm{m}^2 / \mathrm{Vs}] \cdot \mathbf{E} \qquad (9)$$

In the first few tens of µm above the surface in Figure 4c, the field points into the dielectric with a strength of around 10 kV/mm. Such a region with comparatively high field strength and low charge carrier density is typically observed when simulating positive streamer propagation along dielectrics [13]. Its thickness is sensitive to photoemission efficiency as shown in Figure 5. With 10 kV/mm, the positive ion drift speed towards the surface according to equation (9) is around 2 µm/ns. The time needed for the ions to drift onto the surface through the 20-40 µm layer is therefore in the tens of ns, which is fast on a 1.2/50 µs LI timescale. The outer parts of the barrier did not reach saturation before the simulation ended (Figure 3), as they are only exposed to the streamer channel for a few ns.

Charged species are neutralized through recombination, see equation (3) (recombination coefficient $\beta = 2 \times 10^{-13}$ m^3/s [11]). If the recombination in the trailing streamer channel is too fast, the charged species recombine before they can charge the surface to saturation. In the present simulations, the positive species in the quasi-neutral streamer channel are initially being neutralized at a rate of a few 10^{28} /m^{3}s, see Figure 5. As the positive species density behind the streamer head is a few 10^{20} /m^3 (see Figure 5), the charged species will be reduced considerably by recombination during some tens of ns. Nevertheless, saturation charge levels are reached before the charged species in the channel are neutralized in the simulations here.

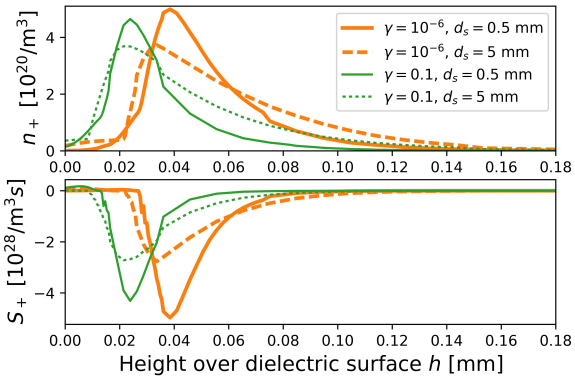

Figure 5 A higher photoemission efficiency γ moves the streamer closer to the dielectric surface. Positive charge species n_+ and source S_+ (equation (3)) above the dielectric surface shown, $d_s = 0.5$ mm and $d_s = 5$ mm behind the streamer head. The source is negative since positive species are recombining in the channel. The streamer has propagated 10 mm along the barrier surface (same as in Figure 6). Geometry G1.

5.2 EFFECT OF PHOTOEMISSION

Photons release electrons from the surface in a highly localized region near the streamer head, where the photons are produced (see green solid line in Figure 6). The surface charging contribution from ion drift (dotted lines in Figure 6) therefore dominates in most of the streamer channel. A higher photoemission efficiency γ leads to a quicker charging of the surface (see Figure 3a). Also, the streamer moves closer to the surface (see Figure 5). Therefore, the ion flux into the surface

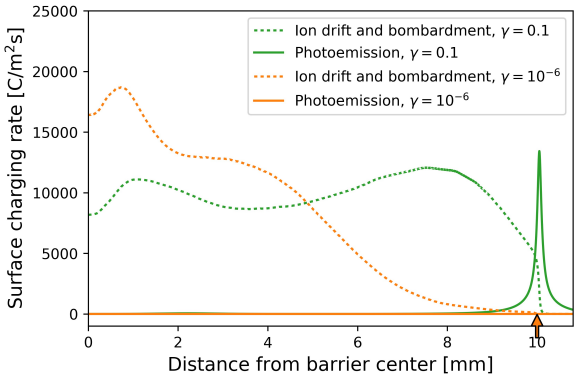

Figure 6 Surface charging by photons (solid lines) is dominant at the streamer head when γ = 0.1, but charging by ion drift (dotted lines) dominates in the rest of the streamer channel. Small vertical arrow indicates streamer head position, which is at 10 mm from the barrier center. $\gamma = 0.1$: t = 8.7 ns, green lines. $\gamma = 10^{-6}$: t = 9.9 ns, orange lines. Geometry G1.

is higher in first few mm behind the head of the streamer channel when γ = 0.1 (see green dotted line vs. orange dotted line within the distance range 5-10 mm in Figure 6). With γ = 10^{-6}, charging by photoemission is negligible along the whole streamer path (orange solid line).

5.3 STREAMER VELOCITY AND STABILITY FIELD

Streamer velocities from 0.1 up to a few mm/ns are typical experimental values in high voltage literature [10], [23], and similar velocities are seen here (see Figure 7 and 8). The velocities increase with voltage and decrease with distance from the live electrode. Positive streamers generally move faster along insulating surfaces than in air, and it has been suggested that photoemission is responsible for this effect [23]. The streamer speed in geometry G1 is a few percent higher when γ = 0.1 than when γ = 10^{-6}. Another explanation for increased streamer velocity along insulating surfaces in uniform fields is that surface streamers are thinner (Figure 7). This promotes a higher streamer head field, and therefore higher ionization intensity and streamer velocity. In the non-uniform fields used here, however, the streamer slows down along the insulator, as it is moving into regions with low background fields (Figure 7 and 8).

The accuracy of the velocity computation for a streamer propagating along a dielectric surface is sensitive to mesh size. An acceptable accuracy level has been observed for mesh size in the range of 1 µm [14]. Reduction of the mesh size below

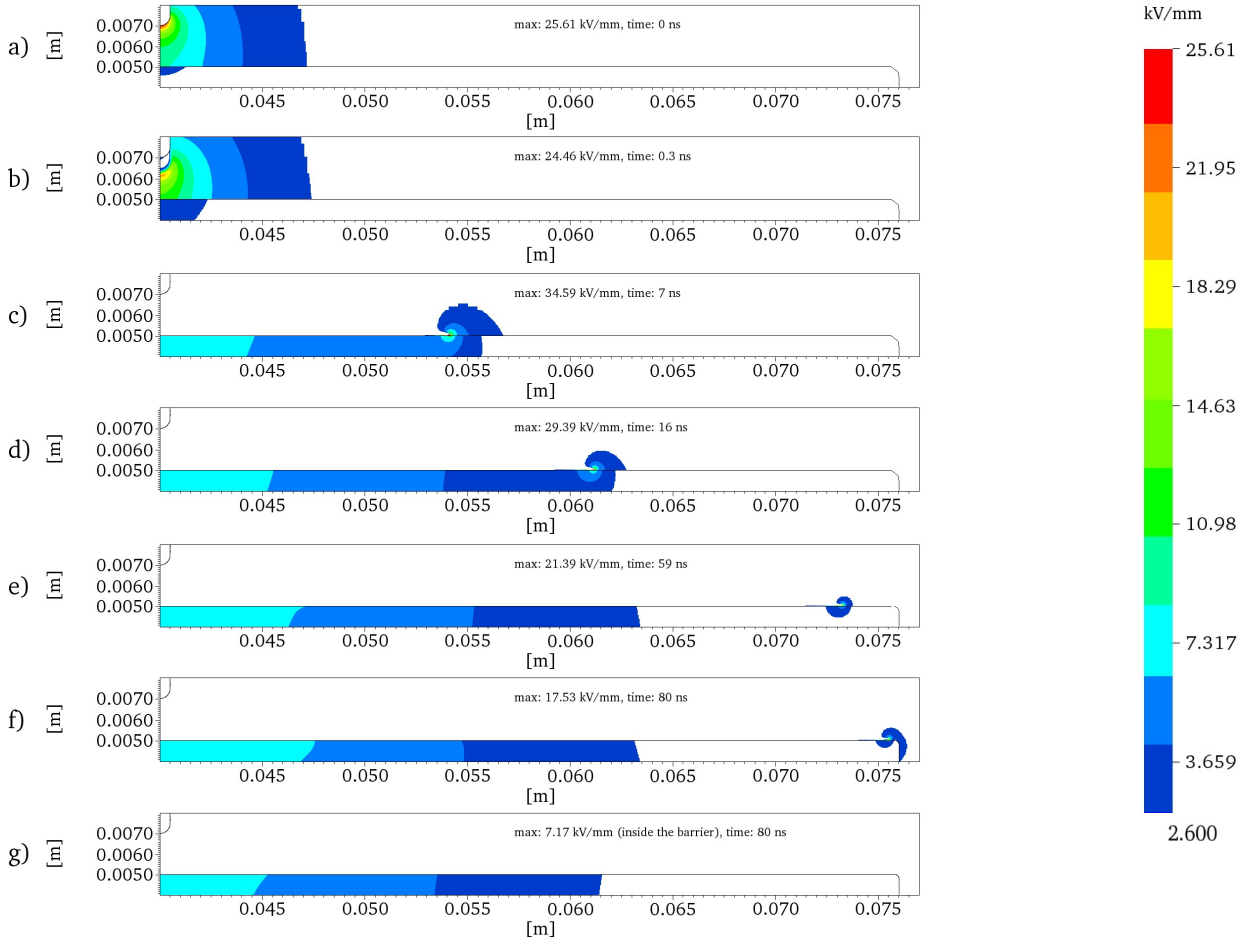

Figure 7 Electric field strength along streamer propagation path for geometry G2, U = 35 kV: a) t = 0 ns (background field), b) t = 0.3 ns (streamer initiated from the blade tip, propagating towards the barrier), c) t=7 ns (streamer propagation along barrier) d) t = 16 ns, e) t = 59 ns, f) t = 80 ns (streamer at the barrier edge) g) electric field after removing the space charge and restarting the simulation at 80 ns (the surface charge is shielding the blade tip, see section 4.5), The field is only plotted in regions where $|\mathbf{E}| \geq 2.6$ kV/mm. Maximum field strength indicated in each plot. The maximum field strength in air is located at the streamer head. Note: As the streamer propagates along and charges the barrier, the electric field strength in air behind the streamer head is reduced below the ionization threshold in air E_{cr} = 2.6 kV/mm (except in the 20-40 µm thin high-field region between the streamer and the surface discussed in section 4.2).

1 µm does not significantly improve accuracy. In the present work a minimum size of 0.61 µm is used.

According to the stability field rule (equation (8)) the streamer in the 14 kV simulation cannot propagate over a distance larger than 28 mm. Consequently, the saturation charge condition has been applied along the barrier surface up to this distance only (red solid curve in Figure 3b). The 14 kV simulation could not be run long enough to confirm that the streamer stops at 28 mm (Figure 8).

However, it can be assumed that the streamer will continue to slow down, as in the 35 kV simulation. Even if it keeps the same speed as it had at the simulation end, it will reach the stability limit for the 14 kV simulation after ca. 400 ns. Considering that the streamer will likely slow down further, it may reach a distance close to the 28 mm limit predicted from equation (8) in a few µs, which fits in to the timescale of 1.2/50 µs LI. Such arrested streamers along insulating surfaces due to low background fields have been observed in pulse voltage experiments [23]. Furthermore, the radius of the surface charged region after a 1.2/50 µs LI was well approximated with equation (8) in [1].

Another confirmation of the stability field concept is provided in the results shown in Figure 9. The average field gradient along the first 15 mm of the surface streamer is 1.2 kV/mm for the 35 kV case, and 0.35 kV/mm for the 14 kV case. Gradient values lower than 0.5 kV/mm indicate that the positive streamer stagnates, and its propagation may stop before reaching the opposite electrode.

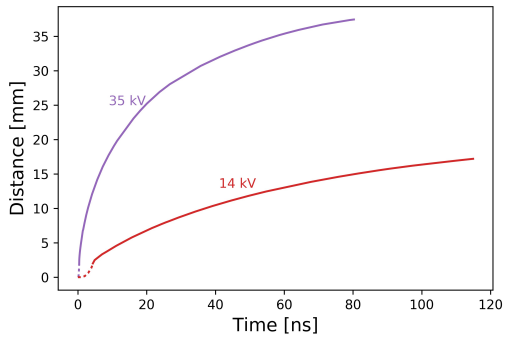

Figure 8 Streamer distance vs time, geometry G2. The 35 kV streamer reaches the barrier edge, but the 14 kV simulation was not run for long enough, and slows down significantly, in support of the stability field concept (equation (8)). Dotted lines indicate propagation in the air gap, solid lines along the barrier.

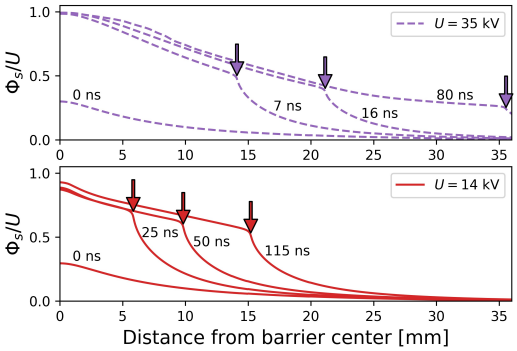

Figure 9 Potential drop along the surface streamer. Surface potential Φ_s on the dielectric surface, normalized to electrode potential U . Elapsed time in ns indicated on each curve. Streamer head position indicated with arrows. Upper plot 35 kV, lower plot 14 kV. Geometry G2.

5.4 DISCHARGE SUPPRESSION BY SURFACE CHARGE

The accumulated surface charge on dielectric barriers can contribute to the LI strength of the insulation system if the exposed points are shielded sufficiently by the streamer-deposited surface charge. Streamers do not automatically cause breakdown, even if they reach the opposite electrode [3]–[5]. If the first streamer does not induce breakdown, the surface charge it deposits on dielectric surfaces may inhibit further discharge activity. The streamer channel will then decay and eventually disappear, leaving surface charge but zero space charge (the surface charge needs a few hours to decay considerably [1]).

Discharge suppression by streamer-deposited surface charge was observed in experiments by the authors (see [1], [3] for description of the experimental setup). For some rod-barrier-plane configurations, an initial LI produced inception (observable with current and surface charge measurements, photo-multipliers and cameras) but additional LIs without discharging and cleaning the surface would not lead to inception.

This effect was investigated in the present work as well. Starting a new simulation with the same initial conditions (resetting the volume charge to a uniform, neutral distribution of 10^{10} m^{-3}), but with the acquired surface charge distribution at the end of the 35 kV simulation (see Figure 7g) did not lead to new discharges, as the field was below the ionization threshold everywhere in air. The field reduction in air due to streamer propagation is evident in Figure 7. As the streamer propagates along the barrier, it shifts the initial high-stress region around the blade tip (Figure 7a) to the insulator and to the streamer head (Figures 7b-7f). The ionization is therefore only sustained near the streamer head and directly behind the head in the thin high-field region between the channel and surface (see section 4.2 and Figure 4c).

Whether and how the streamer-deposited surface charge can inhibit breakdown mechanisms such as leader inception is not investigated here. The streamer-deposited surface and space charge will likely play an important role, as it alters the field distribution considerably [5] (see also Figure 7) .

5.5 BACK DISCHARGE (NEGATIVE STREAMER)

Starting a new simulation with initial conditions for volume charge, but with the acquired surface charge and a grounded HV electrode can lead to a back discharge (negative streamer) initiating from the grounded blade tip. Such a simulation is shown in Figure 10, where the surface charge distribution of the 14 kV geometry G2 simulation is used. Back discharges have also been observed experimentally under LI conditions [1], [6]. They are not disruptive, but they affect the surface charge distribution. Both the resulting volcano-shaped surface potential and negative charging beneath the electrode presented in Figure 10 have been observed in experiments (see Figure 1 and references [1], [6]). Negative streamers (like the back discharge simulated here) differ from positive ones in a number of ways. Importantly, they attach to the surface, leaving no high-field region between the streamer channel and surface. An analysis of the surface charge dynamics of negative streamers is, however, left to another study.

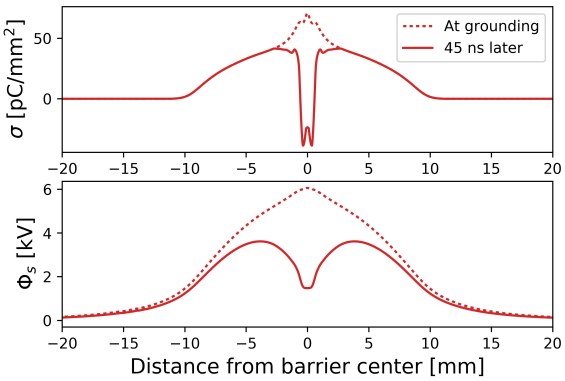

Figure 10 Grounding the blade electrode after removing the space charge (but keeping surface charge) results in negative streamer inception from the blade tip, which changes the surface charge density σ (upper plot) and surface potential Φ_s (lower plot). The resulting characteristic volcano-shaped surface potential is qualitatively consistent with experiments (see Figure 1). Geometry G2,14 kV. Grounding $t = 61.2$ ns after simulation start.

6 CONCLUSIONS AND NEXT STEPS

In this paper, simulations of positive streamer propagation in 2D planar non-uniform electric fields near dielectric barriers are presented. The results obtained using the drift-diffusion model are compared with surface charge predictions by an engineering tool. The engineering tool uses a saturation charge model that has been validated with experiments in simple rod-barrier-plane geometries stressed with lightning impulse voltages. It is shown that the drift-diffusion simulations reproduce the characteristics of the observed charging behaviour. Simulated streamer ranges are consistent with empirical streamer stability field estimates. In the obtained simulation results, ion drift is the dominating surface charge accumulation mechanism, and saturation is achievable within tens of ns. Furthermore, photoemission from the surface increases the charge accumulation rate in the model. Moreover, surface charge deposited by the streamer suppresses further discharge activity in the simulated geometries.

As drift-diffusion simulation models and computer capabilities are improving, such models may become highly useful in dielectric design applications in the near future. Further steps in the development of such models include computation of streamer-dielectric interaction in atmospheric air, in 3D and in larger 2D domains, and improving plasma kinetics models. An important next step is to model surface charging by a single streamer channel in 3D. Other further steps include simulation of negative streamer-dielectric interaction, simulation of leader inception and simulating the influence of surface roughness on streamer-dielectric interaction.

ACKNOWLEDGMENT

This work is part of the project ”Electrical insulation with low-GWP gases” (project number: 245422) funded by the Research Council of Norway and the industrial partners ABB AS, Norway and ABB Switzerland Ltd..

REFERENCES

[1] H. K. Meyer, A. Blaszczyk, M. Schueller, F. Mauseth, and A. Pedersen, “Surface charging of dielectric barriers in short rod-plane air gaps – experiments and simulations,” in *International Conference on High Voltage Engineering and Application (ICHVE)*, Athens, 2018.

[2] A. Pedersen and A. Blaszczyk, “An engineering approach to computational prediction of breakdown in air with surface charging effects,” *IEEE Trans. Dielectr. Electr. Insul.*, vol. 24, no. 5, pp. 2775–2783, Oct. 2017.

[3] H. K. Meyer, F. Mauseth, A. Pedersen, and J. Ekeberg, “Breakdown mechanisms of rod-plane air gaps with a dielectric barrier subject to lightning impulse stress,” *IEEE Trans. Dielectr. Electr. Insul.*, vol. 25, no. 3, pp. 1128–1134, Jun. 2018.

[4] H. Kojima *et al.*, “Classification of impulse breakdown mechanisms under non-uniform electric field in air,” *IEEE Trans. Dielectr. Electr. Insul.*, vol. 23, no. 1, pp. 194–201, Feb. 2016.

[5] I. Gallimberti, G. Marchesi, and L. Niemeyer, “Streamer corona at an insulator surface,” in *7th international symposium on High voltage engineering*, 1991, pp. 26–30.

[6] M. A. Abdul-Hussain and K. J. Cornick, “Charge storage on insulation surfaces in air under unidirectional impulse conditions,” *IEE Proc. - Phys. Sci. Meas. Instrum. Manag. Educ. - Rev.*, vol. 134, no. 9, pp. 731–740, Nov. 1987.

[7] P. Viegas *et al.*, “Investigation of a plasma–target interaction through electric field characterization examining surface and volume charge contributions: modeling and experiment,” *Plasma Sources Sci. Technol.*, vol. 27, no. 9, p. 094002, 2018.

[8] V. R. Soloviev and V. M. Krivtsov, “Surface barrier discharge modelling for aerodynamic applications,” *J. Phys. Appl. Phys.*, vol. 42, no. 12, p. 125208, 2009.

[9] I. Gallimberti, “The mechanism of the long spark formation,” in *Journal De Physique, Colloquium C*, 1979, vol. 7, pp. 193–250.

[10] A. Küchler, *High Voltage Engineering: Fundamentals-Technology-Applications*. Springer, 2017.

[11] R. Morrow and J. J. Lowke, “Streamer propagation in air,” *J. Phys. Appl. Phys.*, vol. 30, no. 4, p. 614, 1997.

[12] B. Bagheri *et al.*, “Comparison of six simulation codes for positive streamers in air,” *Plasma Sources Sci. Technol.*, 2018.

[13] V. R. Soloviev and V. M. Krivtsov, “Mechanism of streamer stopping in a surface dielectric barrier discharge,” *Plasma Phys. Rep.*, vol. 40, no. 1, pp. 65–77, Jan. 2014.

[14] W. Hua and K. Fukagata, “Influence of grid resolution in fluid-model simulation of nanosecond dielectric barrier discharge plasma actuator,” *AIP Adv.*, vol. 8, no. 4, p. 045209, Apr. 2018.

[15] S. Singh and Y. V. Serdyuk, “Simulations of Nonthermal Electrical Discharges in Air Over Solid Insulating Barrier,” *IEEE Trans. Plasma Sci.*, pp. 1–7, 2018.

[16] R. Marskar, “An adaptive Cartesian embedded boundary approach for fluid simulations of two- and three-dimensional low temperature plasma filaments in complex geometries,” *ArXiv180903745 Phys.*, Sep. 2018.

[17] R. Marskar, “Adaptive multiscale methods for 3D streamer discharges in air,” *Plasma Res. Express*, vol. 1, no. 1, p. 015011, Jan. 2019.

[18] F. Pechereau, J. Jánský, and A. Bourdon, “Simulation of the reignition of a discharge behind a dielectric layer in air at atmospheric pressure,” *Plasma Sources Sci. Technol.*, vol. 21, no. 5, p. 055011, 2012.

[19] G. E. Georghiou, A. P. Papadakis, R. Morrow, and A. C. Metaxas, “Numerical modelling of atmospheric pressure gas discharges leading to plasma production,” *J. Phys. Appl. Phys.*, vol. 38, no. 20, p. R303, 2005.

[20] A. Bourdon, V. P. Pasko, N. Y. Liu, S. Célestin, P. Ségur, and E. Marode, “Efficient models for photoionization produced by non-thermal gas discharges in air based on radiative transfer and the Helmholtz equations,” *Plasma Sources Sci. Technol.*, vol. 16, no. 3, p. 656, 2007.

[21] S. Pancheshnyi, “Role of electronegative gas admixtures in streamer start, propagation and branching phenomena,” *Plasma Sources Sci. Technol.*, vol. 14, no. 4, p. 645, 2005.

[22] A. A. Dubinova, “Modeling of streamer discharges near dielectrics,” TU Eindhoven, 2016.

[23] N. L. Allen and P. N. Mikropoulos, “Streamer propagation along insulating surfaces,” *IEEE Trans. Dielectr. Electr. Insul.*, vol. 6, no. 3, pp. 357–362, Jun. 1999.